Electric measurement and magnetic control of spin transport in InSb-based lateral spin devices

N. A. Viglin,[1,*] V. V. Ustinov,[1,2] S. O. Demokritov,[1,3] A. O. Shorikov,[1,2] N. G. Bebenin,[1] V. M. Tsvelikhovskaya,[1] T. N. Pavlov,[1] and E. I. Patrakov[1]

[1]*Institute of Metal Physics, Ekaterinburg 620990, Russia*

[2]*Institute of Natural Sciences, Ural Federal University, Ekaterinburg 620083, Russia*

[3]*Institute for Applied Physics and Center for Nonlinear Science, University of Muenster, 48149 Muenster, Germany*

(Received 25 October 2017; published 7 December 2017)

Electric injection and detection of spin-polarized electrons in InSb semiconductors have been realized in nonlocal experimental geometry using an InSb-based "lateral spin valve." The valve of the InSb/MgO/$Co_{0.9}Fe_{0.1}$ composition has semiconductor/insulator/ferromagnet nanoheterojunctions in which the thickness of the InSb layer considerably exceeded the spin diffusion length of conduction electrons. The spin direction in spin diffusion current has been manipulated by a magnetic field under the Hanle effect conditions. The spin polarization of the electron gas has been registered using ferromagnetic $Co_{0.9}Fe_{0.1}$ probes by measuring electrical potentials arising in the probes in accordance with the Johnson-Silsbee concept of the spin-charge coupling. The developed theory is valid at any degree of degeneracy of electron gas in a semiconductor. The spin relaxation time and spin diffusion length of conduction electrons in InSb have been determined, and the electron-spin polarization in InSb has been evaluated for electrons injected from $Co_{0.9}Fe_{0.1}$ through an MgO tunnel barrier.

DOI: 10.1103/PhysRevB.96.235303

I. INTRODUCTION

The goal of many years of research in semiconductor spintronics is to realize electrically injecting and detecting spin-polarized electrons in a single device [1,2]. The use of semiconductors as a medium for spin transport is extremely attractive because of their broad functionality, not realized in metallic systems. The equilibrium carrier densities can be varied over a wide range by doping. Furthermore, as the typical carrier densities in semiconductors are low as compared to those of metals, the electronic properties of the former are easily adjusted by gate potentials [3]. However, a lower concentration of electrons in semiconductors is the cause of the conductivity mismatch problem, i.e., the efficiency of spin injection into a semiconductor from a ferromagnetic metal dramatically reduces due to a significant difference in conductivity of metals and semiconductors [4]. Theoretically, the mismatch problem can be balanced by creating a tunnel barrier between a metal injector and a semiconductor, as the spin-dependent barrier resistance is comparable to the spin-independent resistance of a normal metal [5,6]. In this case, the spin injection efficiency increases, and the spin polarization of conduction electrons in the semiconductor may be commensurable with the magnitude of the spin polarization of electrons in the ferromagnetic injector [7].

Electrical detection of spin-polarized electrons injected into a semiconductor is a quite difficult task. Recently, it has become possible to detect the spin polarization of the electron gas in a thin film of a nonferromagnetic metal or a semiconductor using metal ferromagnetic probes located on the film surface. This method has gained a great popularity, and the appropriate devices are referred to as lateral spin valves. The electric potential that arises on the ferromagnetic contact in such a device when spin nonequilibrium electrons appear in the semiconductor is determined by the nonequilibrium magnetization of the electron gas in the nonferromagnet under the contact and by the electron magnetization of the contacts themselves. The theory that explains the sensitivity of the ferromagnetic probes to the electron gas magnetization in the nonferromagnet near these electrodes was proposed by Johnson and Silsbee [8,9] and developed in [7,10,11].

Over the past few years, several semiconductor spintronic devices with electrical detection of spin-polarized electrons have been designed. Injection and detection were brought about in:

(i) GaAs thin film with a Fe injector [11] and an injector of a magnetic semiconductor (Ga, Mn)As [12];

(ii) Si thin film with permalloy ($Ni_{80}Fe_{20}$) contacts and tunnel barriers of SiO_2 and graphene [13];

(iii) InSb plate with Fe ferromagnetic electrodes and an MgO tunnel barrier between the electrodes and the semiconductor [14].

In this work we investigate the spin injection into an InSb plate but in contrast to Ref. [14], we exploit $Co_{0.9}Fe_{0.1}$ ferromagnetic alloy rather than Fe as a material for the injector and detector because $Co_{0.9}Fe_{0.1}$ with MgO tunnel barrier can produce higher spin polarization than Fe [15].

The theoretical expressions published in [7–9] are applicable for the degenerate gas only. Our devices, however, contain an n-InSb plate in which electron gas is nondegenerate. For this reason, in the next section we derive formulas that are valid at an arbitrary degree of degeneracy. Also we try to take into account the fact that electrons are injected into a rather thick plate, i.e., in fact bulk material, which results in the weakening of the detected spin polarization as compared with the case of the very thin semiconductor films.

It should be noted that indium antimonide has an extremely small effective mass and records high electron mobility ($\mu \sim 10^6\,\mathrm{cm}^2/(\mathrm{Vs})$ in n-InSb with an electron density of about $10^{14}\,\mathrm{cm}^{-3}$ [16]). Such materials are quite interesting for studying phenomena related to spin transport. In this context, the publication [17] should be mentioned, the authors of which

*Author to whom correspondence should be addressed: viglin@imp.uran.ru

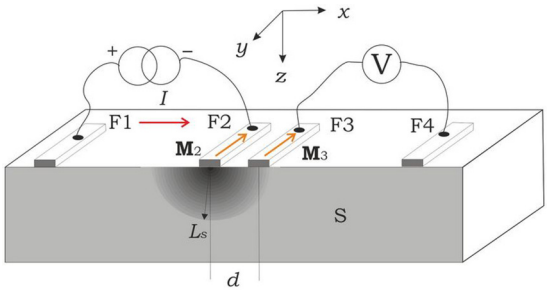

FIG. 1. Scheme of a device for injection and detection of spin-polarized electrons with the ferromagnetic contacts F1–F4 in a paramagnetic semiconductor S. Contacts F1 and F2 are current and contacts F3 and F4 are potential ones located outside the current circuit ("nonlocal" experimental geometry).

demonstrate the possibility of creating a spin injection maser that generates terahertz radiation with a frequency tunable by a magnetic field.

II. THEORETICAL BACKGROUND

The spin polarization to be detected in the device requires a built-in miniature detector the dimensions of which must be smaller than the spin diffusion lengths L_S. The distance d between the injector and the spin detector must be of the same order $d \leqslant L_S$. This circumstance imposes rigid restrictions on the scales of such devices. It should be noted that for most pure nonferromagnetic metals, the spin diffusion length L_S even at a temperature of $T = 4.2\,\mathrm{K}$ amounts to fractions of micrometers [18], except probably only for Al, the L_S of which exceeds tens of micrometers [8]. In semiconductors, due to a significantly lower electron density and greater mobility of electrons as compared to metals, the spin diffusion length can reach unities and tens of micrometers. For example, in GaAs, the spin diffusion length at $T = 50\,\mathrm{K}$ was determined as $L_S = 6\,\mu\mathrm{m}$ [11]. Thus, the requirements for the maximum dimensions of the devices for electrical detection of polarized electrons in semiconductors remain quite stern.

The simplest device for electrically observing spin transport phenomena consists of four ferromagnetic narrow strip-shaped electrodes arranged parallel to each other on the surface of a nonferromagnetic semiconductor (Fig. 1). The conduction electrons of the ferromagnet are assumed to have nonzero spin polarization, for example, due to internal exchange interaction with the magnetically ordered system of localized electrons. Also, the width of the strips is suggested to be less than the spin diffusion length L_S.

The contacts are magnetized and have a residual magnetization $\mathbf{M}_i, i = 1$–4. Electric current I flows from the contact F1 to the contact F2 through the semiconductor S. The contact F2 plays here the role of the injector of electrons that carry a charge of $(-e)$. In the semiconductor under F2 there arises a cloud of polarized electrons with the polarization degree of less than (or, ideally, equal to) the polarization of the injector electrons. It is generally agreed that the spin accumulation is observed in the contact region [3]. As the distance from the contact injector in any direction increases, the degree of polarization of the electron gas subsides, and the parameter L_S characterizes this decrease. The detector (contact F3) is located outside the circuit of current I at a distance d from the injector F2. The distance d is commensurate with L_S. This experimental geometry is called "nonlocal" due to registering the nonequilibrium spin density of electrons diffusing *outside* the electric current circuit. According to the Johnson-Silsbee concept [8,9], the nonequilibrium spin density of electrons in S induces a change of the contact potential difference in the ferromagnetic-semiconductor system. The contact potential difference of the S-F3 pair differs from that of the S-F4 pair distanced from the injector by a space considerable exceeding L_S. Consequently, a voltage V_D determined by the spin accumulation near the detector F3 arises between F3 and F4.

The spin accumulation is described as a deviation of the spin-dependent conduction electron densities of a ferromagnet and a nonferromagnet from equilibrium values. This deviation causes local changes in the chemical potential of the spin subsystems of the contact pairs, and, as a result, the local changes of the contact potential difference in the "ferromagnet/nonferromagnet" system. In calculations of the V_d voltage, the electron density deviation in the spin subsystems from equilibrium for both the ferromagnet and the nonferromagnet must be estimated, and the deviations of the spin densities must be related to the deviation from equilibrium of chemical potentials of the spin subsystems. In doing so, the law of charge carrier dispersion in these materials should be set out. Until now, the estimates were performed for spin valves in which a ferromagnetic detector and a nonferromagnet were materials with degenerate electron gas [10–12]. The most detailed calculation of the voltage induced by spin accumulation in a degenerate semiconductor was done in Ref. [7].

For further consideration, we give main relations of the Johnson-Silsbee spin-charge coupling; their form allows describing the spin valves made of materials with arbitrary dispersion of charge carriers and an arbitrary degree of degeneracy of the electron gas in a nonferromagnet.

First, we find a change in the contact potential difference on the ferromagnetic detector F due to the deviation of the spin system from equilibrium in the contact pair S-F. Suppose the equilibrium spin polarization $P_S^{(\mathrm{F})}$ of the conduction electrons in the ferromagnet F to be nonzero. Its value in the contact depth (a distance from the interface exceeds the Debye screening length) is defined as

$$P_S^{(\mathrm{F})} = \frac{n_+^{(\mathrm{F})} - n_-^{(\mathrm{F})}}{n_+^{(\mathrm{F})} + n_-^{(\mathrm{F})}}, \tag{1}$$

where $n_\lambda^{(\mathrm{F})}$ is the equilibrium electron density in the depth of the ferromagnetic contact F with spin λ, and index λ takes two values: $\lambda = +$ for the spin-up electrons and $\lambda = -$ for the spin-down electrons. In this case, the spin quantization axis is chosen along the y axis. The quantity $S^{(\mathrm{F})} = n_+^{(\mathrm{F})} - n_-^{(\mathrm{F})}$ is the y component of the vector of the electron spin density measured in units of $\hbar/2$, where $\hbar$ is Planck's constant. The quantity $n_\mathrm{F} = n_+^{(\mathrm{F})} + n_-^{(\mathrm{F})}$ is the equilibrium density of electrons in ferromagnet F.

At the thermodynamic equilibrium, the value of the electron density $n_\lambda^{(\mathrm{F})}$ in the ferromagnet is related to the value of

the chemical potential ζ in the nonferromagnet/ferromagnet system as

$$n_\lambda^{(\mathrm{F})} = \sum_{\mathbf{p}} F\left(\varepsilon_{\mathbf{p}\lambda}^{(\mathrm{F})} - e\phi - \zeta\right), \tag{2}$$

where $\varepsilon_{\mathbf{p}\lambda}^{(\mathrm{F})}$ is the energy spectrum of charge carriers in the ferromagnet with the quasimomentum $\mathbf{p}$ and spin λ, ϕ is the contact potential difference of the nonferromagnet/ferromagnet system, $-e$ is the electron charge, and $F(E) = 1/[\exp(E/k_\mathrm{B}T) + 1]$ is the Fermi function, k_B is Boltzmann's constant, and T is temperature.

Let the spin subsystems of the ferromagnet be disturbed from a mutual thermodynamic spin equilibrium by an external influence. The unbalance gives rise to a change in the contact potential difference of the nonferromagnet/ferromagnet system by the magnitude of $\delta\phi$. However, each of the spin subsystems comes to a quasimomentum equilibrium characterized by local-equilibrium values of the chemical potential. Let us designate these local-equilibrium quantities as $\zeta_\lambda = \zeta + \delta\zeta_\lambda$. The quantity ζ_λ often called the quasichemical potential [7] is responsible for the deviation of the chemical potential of the electron spin system with λ from the equilibrium value. The deviation $\delta\zeta_\lambda$, the change $\delta\phi$, and the nonequilibrium addition $\delta n_\lambda^{(\mathrm{F})}$ to the electron density are related together by

$$n_\lambda^{(\mathrm{F})} + \delta n_\lambda^{(\mathrm{F})} = \sum_{\mathbf{p}} F\left(\varepsilon_{\mathbf{p}\lambda}^{(\mathrm{F})} - e\phi - e\delta\phi - \zeta - \delta\zeta_\lambda\right). \tag{3}$$

For small deviations from the local equilibrium, the nonequilibrium addition appears as

$$\delta n_\lambda^{(\mathrm{F})} = \frac{\partial n_\lambda^{(\mathrm{F})}}{\partial\zeta}(\delta\zeta_\lambda + e\delta\phi). \tag{4}$$

In the balanced nonferromagnet, the spectrum of the charge carries is spin independent and can be defined by the single function $\varepsilon_\mathbf{p}$. The densities of the spin-up and spin-down electrons are equal, $n_+ = n_- = n/2$, and n is the equilibrium charge-carrier density in the nonferromagnet:

$$n = 2\sum_{\mathbf{p}} F(\varepsilon_\mathbf{p} - \zeta). \tag{5}$$

As well as for the ferromagnet, the small deviations δn_λ of the electron densities from their equilibrium in the spin subsystems of the nonferromagnet can be written as

$$\delta n_\lambda = \frac{1}{2}\frac{\partial n}{\partial\zeta}\delta\zeta_\lambda. \tag{6}$$

Let $S = \delta n_+ - \delta n_-$ be the nonequilibrium spin density of the nonferromagnet. Assuming that the electrical neutrality condition $\delta n_+^{(\mathrm{F})} + \delta n_-^{(\mathrm{F})} = 0$ is fulfilled outside the contact region, we can derive the following relation from the system of equations (6):

$$\delta\zeta_+ = -\delta\zeta_- = S\left(\frac{\partial n}{\partial\zeta}\right)^{-1}. \tag{7}$$

Utilizing this condition as well as relation (7), we can solve the system of Eq. (4) and calculate the dependence of the magnitude of the change in the contact potential difference $\delta\phi$ on the nonequilibrium electron spin density of the nonferromagnet S:

$$\delta\phi = -\frac{1}{e}A_\mathrm{F}\left(\frac{\partial n}{\partial\zeta}\right)^{-1} S. \tag{8}$$

In (8) we have introduced the spin asymmetry parameter A_F of the ferromagnet, defined by the expression

$$A_\mathrm{F} = \frac{\frac{\partial n_+^{(\mathrm{F})}}{\partial\zeta} - \frac{\partial n_-^{(\mathrm{F})}}{\partial\zeta}}{\frac{\partial n_+^{(\mathrm{F})}}{\partial\zeta} + \frac{\partial n_-^{(\mathrm{F})}}{\partial\zeta}}. \tag{9}$$

The value of the spin asymmetry parameter A_F of the ferromagnet can be calculated by setting the energy spectrum of electrons $\varepsilon_{\mathbf{p}\lambda}^{(\mathrm{F})}$. The spin-up and spin-down electron densities $n_+^{(\mathrm{F})}$ and $n_-^{(\mathrm{F})}$ appearing in (9) determine the total density of the charge carriers in the ferromagnet $n_\mathrm{F} = n_+^{(\mathrm{F})} + n_-^{(\mathrm{F})}$, as well as the electron polarization P_F. Substituting the above expressions for the densities $n_\pm^{(\mathrm{F})} = n_\mathrm{F}(1 \pm P_S^{(\mathrm{F})})/2$ into (9), we arrive at the formula for A_F in terms of spin polarization $P_S^{(\mathrm{F})}$ of the ferromagnet:

$$A_\mathrm{F} = P_S^{(\mathrm{F})}\left[1 + n_\mathrm{F}\frac{\partial}{\partial n_\mathrm{F}}\ln\left|P_S^{(\mathrm{F})}\right|\right]. \tag{10}$$

The logarithm of the polarization in expression (10) is weakly dependent on the electron density n_F. Then the expression in the square brackets of Eq. (10) is close to unity and $A_\mathrm{F} \approx P_S^{(\mathrm{F})}$, and in further consideration this approximation is used.

Let us define the electron polarization in the nonferromagnet as $P_S(x) = S(x)/n$. Then Eq. (8) takes the simple form

$$\delta\phi(x) = -\frac{1}{e}P_S^{(\mathrm{F})}P_S(x)\frac{n}{\frac{\partial n}{\partial\zeta}}. \tag{11}$$

The dependence of $\delta\phi$ on the parameters of the semiconductor electronic system is determined by the factor $(n/\frac{\partial n}{\partial\zeta})$. Equation (11) can be utilized for analyzing spin injection from a ferromagnetic metal into a semiconductor with any degree of degeneracy of the electron gas of the latter. For a degenerate electron gas, the value of $(n/\frac{\partial n}{\partial\zeta})$ coincides with the Fermi energy up to a numerical factor of the order of unity. For a nondegenerate gas, this value is equal to $k_\mathrm{B}T$.

From the spin diffusion equation, it follows that the spin density $S(x)$ and the polarization $P_S(x)$ in the nonferromagnet fall off exponentially with distance from the injector. If the distance $x = d_{23}$ between the injector F2 and the detector F3 (Fig. 1) is comparable to the electron spin-diffusion length L_S in the nonferromagnet, then $P_S(d_{23})$ is nonzero and the electric potential at the contact F3 is $\Phi_3 = \phi + \delta\phi(d_{23})$. Its value differs from the equilibrium contact potential difference ϕ. The contact F4 in the detector circuit is far away from F2 by a distance $d_{24} \gg L_\mathrm{S}$. The spin polarization magnitude $P_S(d_{24})$ at such a distance is exponentially small and the electric potential at the contact F4 is equal to the equilibrium one $\Phi_4 \approx \phi$. Then the potential difference V_{34} measured between the F3 and F4 contacts amounts to $V_{34} = \Phi_3 - \Phi_4 = \delta\phi(d_{23})$.

Expression (11) was derived under the assumption that the spin quantization axis is directed along the y axis. We denote

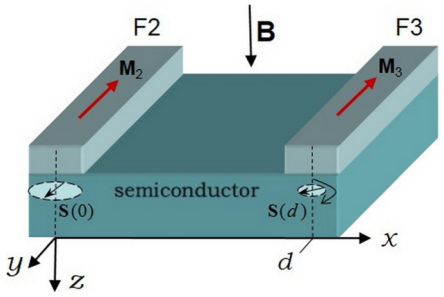

FIG. 2. Scheme of spin injection under the Hanle effect in a lateral spin valve. $\mathbf{S}(0)$ is the spin density of electrons injected from contact F2. $\mathbf{S}(d)$ is the spin density of electrons diffused from injector F2 to detector F3.

the voltage on the detector as $V_D(d)$, where d is the distance between the center axes of the injector and detector. To describe the experiments for measuring $V_D(d)$ with different mutual orientations of the injector and detector magnetization vectors, it is convenient to employ local quantization axes associated with the direction of these vectors. With a choice of the local quantization axis along the direction of the equilibrium spin density in the ferromagnetic contact at hand, the polarization $P_S^{(\mathrm{F})}$ becomes a positive quantity, and the expression for $V_D(d)$ acquires the form

$$V_D(d) = \mp\frac{1}{e}P_S^{(\mathrm{F})}\left(\frac{\partial n}{\partial \zeta}\right)^{-1} S_y(d), \tag{12}$$

where $S_y(d)$ is the y component of the spin density vector $\mathbf{S}(x)$ at the point $x = d$. The choice of the sign $\mp$ in expression (12) depends on the mutual directions of the injector and detector magnetizations. A negative voltage arises on the detector as the injector and the detector are parallel magnetized. If the magnetization directions of the detector and injector are opposite, the voltage sign is positive.

Formula (12) explicitly demonstrates the possibility of electrical detection of a spin signal due to a change in the mutual orientation of the injector and the detector magnetizations. When electrically detecting the spin diffusion, the nonlocal voltage $V(d)$ needs to be measured under parallel and antiparallel magnetization of the injector and detector. For this purpose, the contacts lying in the plane of the device should be reversed magnetized by a magnetic field. However, if the magnetization reversal causes the domain structure with different directions of magnetization in the domains, the measurements of $V_D(d)$ provide ambiguous results using such a detection method.

The spin-induced electrical signal can be more reliably and unambiguously registered by changing the direction of the vector of the electron spin density $\mathbf{S}(x)$. At the same time, the magnetization directions of the injector and detector are preassigned and unvaried. The direction of the vector of the electron spin density $\mathbf{S}(x)$ can be changed by a transverse magnetic field. The impact applied should be perpendicular to the magnetization of the injector and act on the magnetization of the polarized electron gas injected into the nonferromagnet. This is the so-called Hanle effect (Fig. 2).

The spins of electrons which diffuse from the injector to the detector in a transverse magnetic field $\mathbf{B}$ directed along the z axis rotate by an angle $\Omega_L t$ for a time t. Here $\Omega_L = \mathrm{g}\,\mu_B B/\hbar$ is the Larmor frequency, g is the Lande factor of conduction electrons, μ_B is the Bohr magneton, and $\hbar$ is Planck's constant. Under the assumption that the detector is sensitive to the spin projection on the direction of magnetization in it, the contribution of each electron to the output signal is proportional to $\cos(\Omega_L t)$. As the electrons have different transit times, their spin precession angles differ. Calculating the contribution from all the electrons at the point of detection requires integrating over all the times of diffusion.

Thus, to calculate the signal $V(d)$, we need to find the profile of the spin density. For this purpose, we use the Bloch-Torrey equation that takes into account the spin precession of the electrons in the magnetic field, the diffusion nature of their motion, and the spin relaxation of conduction electrons:

$$\frac{\partial \mathbf{S}}{\partial t} = \gamma[\mathbf{S}\times \mathrm{B}] + D\nabla^2\mathbf{S} - \frac{1}{T_S}\mathbf{S}. \tag{13}$$

In Eq. (13) $\gamma = \mathrm{g}\,\mu_B/\hbar$ is the gyromagnetic ratio, D is the diffusion coefficient, and T_S is the spin relaxation time. With further consideration, we are interested in the behavior of only the x and y components of the spin density vector $\mathbf{S}$ that precesses relative to the magnetic field vector $\mathbf{B}$ directed along the z axis.

The vector $\mathbf{S}$ is, generally speaking, a function of all three coordinates x, y, and z. To simplify the presentation of the results, we use a one-dimensional model for describing spin diffusion. In doing so, the injected spin density $\mathbf{S}$ is assumed to diffuse along the x axis by the law of Eq. (13) and to decrease over the spin diffusion length L_S. Its decay is described by a simple exponential law. We denote the spin density on the semiconductor surface ($z = 0$) as $\mathbf{S}(x)$.

For Eq. (13) to be unambiguously solved, it is necessary to involve the boundary conditions for spin density $\mathbf{S}(x)$ on the semiaxis $x \geqslant 0$ for $x = 0$. Let w and l be the linear dimensions of the injector contact. The electric current I flowing through the injector has a density $J_C = I/wl$ and causes the spin current with the density J_S to pass through the injector-semiconductor boundary. The spin current density J_S and the particle current density $J = J_C/(-e)$ are related as $J_S = P_J J$. Here, to characterize the injection contact properties, we enter the parameter of the spin-current injection efficiency P_J as $P_J = J_S/J$. The parameter P_J introduced in such a way can also be called the polarization of the spin current.

The spin current $J_S wl$ injected into the semiconductor can be divided into two parts responsible for the spin transfer along the x axis in the $x > 0$ and $x < 0$ directions. For $x > 0$, the flux densities of the x and y components of the spin density $\mathbf{S}$ along the x axis are governed only by spin diffusion: $J_{S_x}(x) = -D\nabla_x S_x(x)$, $J_{S_y}(x) = -D\nabla_x S_y(x)$. For $x < 0$, the flux density of the spin density includes both the diffusion contribution and the conduction-electron drift contribution. The latter depends on the magnitude of the current I. For not too large currents, the drift contribution to the spin current may be neglected and the spin currents flowing along the x axis at $x = +0$ and $x = -0$ are assumed to be equal in absolute value. Suppose that only the y component of the spin density is injected into the semiconductor, while the flux of the x component is zero. From the law of conservation of the

spin moment, we obtain the following boundary conditions for $x = +0$:

$$\nabla_x S_x|_{x=+0} = 0, \quad \nabla_x S_y|_{x=+0} = -\frac{w}{2L_S D} P_J J. \tag{14}$$

Now Eq. (13) can be solved for the $S_y(x)$ and $S_x(x)$ components. Its steady-state solution meets the boundary conditions (14) and the vanishing conditions as $x \to \infty$. If there is no magnetic field, the solution of Eq. (13) under the conditions (14) has a simple exponential form, and the expression for $V_D(d)$ can be written as

$$V_D(d) = \mp\frac{1}{e} P_S^{(\mathrm{F})} P_S \frac{n}{\frac{\partial n}{\partial \zeta}} \exp\left(-\frac{d}{L_S}\right), \tag{15}$$

where

$$P_S = P_J \frac{w\, T_S}{2nL_S^2} J \tag{16}$$

is the spin polarization of conduction electrons in the semiconductor directly under the contact injector.

Omitting the technical details for solving Eq. (13) in the presence of a magnetic field B, we give the result for the dependence of voltage V_D on the distance d, as well as on the magnetic field B:

$$V_D(B,d) = \mp\frac{1}{e} P_S^{(\mathrm{F})} P_S \frac{n}{\frac{\partial n}{\partial \zeta}} \exp\left(-\frac{d}{L_S}\alpha\right) \times \frac{\alpha \cos\left(\frac{d}{L_S}\beta\right) - \beta \sin\left(\frac{d}{L_S}\beta\right)}{\alpha^2 + \beta^2}. \tag{17}$$

In Eq. (17) $L_S = \sqrt{DT_S}$ is the spin diffusion length, and the B-field-dependent parameters α and β characterize the effective spin diffusion length in the magnetic field and the effective period of the spin precession, respectively:

$$\alpha = \sqrt{[\sqrt{1 + (\Omega_L T_S)^2} + 1]/2},$$
$$\beta = \sqrt{[\sqrt{1 + (\Omega_L T_S)^2} - 1]/2}. \tag{18}$$

The magnitudes of the spin polarization P_S of the electrons injected into the semiconductor and the spin-current injection efficiency P_J are parameters of the theory and can be calculated from the experimentally measured signal V_D if the spin diffusion length L_S and the spin relaxation time T_S are already known or obtained earlier from the same experiment. Obviously the polarization P_S depends on the electric current I that flows across the circuit of the injector from F1 into F2 (Fig. 1). The relation (17) reflects explicitly the main mechanisms for describing the dependence of the polarization P_S in the nonferromagnet on the current I flowing through the injector.

To calculate the value of the polarization $P_S^{(\mathrm{F})}$ in the CoFe alloy under consideration, we applied the LDA + U method [19] for describing the electronic structure within the strong-coupling approach in the cellular potential and atomic-sphere approximation (TB-LMTO-ASA) [20]. For modeling the alloy, we considered a supercell consisting of 8 Co atoms, wherein one atom of Co substitutes for a Fe atom. In calculating we used the crystal structure parameters for pure Co (symmetry group $Fm-3m$, $a = 3.5472$ Å). Thus, the model alloy had a $Co_{0.875}Fe_{0.125}$ composition close to experimental $Co_{0.9}Fe_{0.1}$. Calculating in a self-consistent way gives populations of the s, p, d shells with up and down spins for obtaining the polarization value of $P_S^{(\mathrm{F})} = 0.224$ by formula (1).

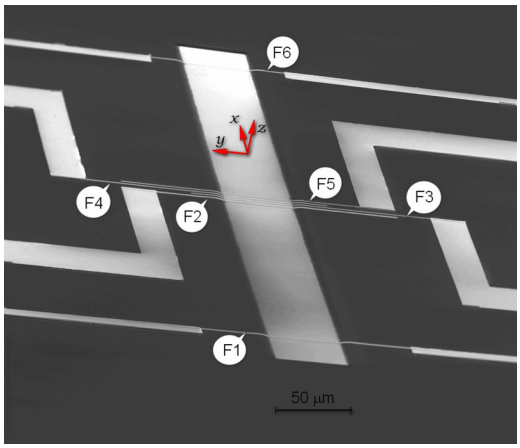

FIG. 3. SEM image of a spin valve used in the experiment. A bright rectangle of 1.4 mm length and 50 μm width in the center is the InSb semiconductor. The ferromagnetic electrodes F1 and F2 (of 6 μm width) and F3, F4, F5, and F6 (of 4 μm width) are made of a $Co_{0.9}Fe_{0.1}$ alloy, and they are separated from the semiconductor by an MgO layer of a thickness of 1.8 nm.

III. EXPERIMENTAL SETUP

Devices for studying spin transport in InSb semiconductors were prepared on square substrates with a side length of 10 mm and a thickness of 0.4 mm, cut from the (100) plate of undoped n-InSb. The surface roughness was measured using an optical profilometer and did not exceed 0.6 nm. The data on concentration of electrons ($n = 1.2\times10^{14}$ cm^{-3}) and their mobility [($\mu = 6.2\times10^5$ cm^2/(Vs) at $T = 77$ K] were taken from a certificate for the semiconductor plate.

Standard photolithography and lift-off techniques are used to determine the semiconductor channel and to pattern the six ferromagnetic electrodes (see Fig. 3), which have nominal dimensions of 6 μm×50 μm (F1, F2) and 4 μm×50 μm (F3, F4, F5, F6). Distances between contacts F1 and F2, F5 and F6 are 0.59 mm. The contacts F3, F4, and F5 have a center-to-center spacing of 10 μm, and F2 and F3 are spaced at 11 μm. The long sides of the contacts are oriented along the ⟨110⟩ crystal axis of the InSb substrate. A photoresist layer of 1 μm thick on the substrate plays a role of an insulating layer. The magnetron sputtering method was used to fabricate the contacts F1–F6. The contact structure is as follows: an MgO dielectric layer of a nominal thickness of 1.8 nm, a $Co_{0.9}Fe_{0.1}$ ferromagnetic metal layer 80 nm thick, and a Ta layer of 3 nm thickness to protect the contacts from oxidation. Finally, the Ni/Cu/Ag vias and bonding pads were fabricated

by magnetron sputtering (by thermal evaporation for the Ag layer) and lift-off.

The magnitude of the electrical signal arising on the detector depends on the distance d between the injector and the detector. To change d, we can produce various combinations of the contacts in our device (see Fig. 3). For example, any of the contacts F3, F4, and F5 can be used as a voltage detector relative to the outlying electrode F6. The contacts F2, F3, or F4 can be applied as an injector of polarized electrons. For that, a constant current is passed between one of the contacts and the contact F1. The magnitude and sign of the signal also depend on the electron polarization P_S in the semiconductor. In turn, P_S is related to the magnitude of the injector current I. In our experiments, we could vary the magnitude and direction of the current I. The experimental setup consists of a dc current source based on alkaline batteries, a nanovoltmeter, and an electromagnet equipped with a cryostat and a programmable power supply. The measurements were carried out at a temperature of 77 K.

The ferromagnetic contacts were initially magnetized by a magnetic field of 1 kG directed along the y axis. Then the field value was reduced to that close to zero, and the entire device was rotated in the cryostat by 90° so that the field direction should be perpendicular to the contact plane. When registering the Hanle effect, the transverse magnetic field B was scanned slowly in the range of ±20 G. It should be noted that the magnitudes of these fields are much smaller than those of the transverse anisotropy field of a flat ferromagnetic contact, its value for the $Co_{0.9}Fe_{0.1}$ film being about 15 kOe. Therefore, they exert no significant influence on the longitudinal magnetization of the contacts.

IV. RESULTS AND DISCUSSION

The sign of the electrical signal on the detector V_D depends on the mutual orientation of the electron gas and detector magnetizations. In turn, the magnetization direction of the injected electrons is defined by the magnetization of the injector. Thus, a correct measurement of the spin effects requires uniformly magnetizing both the injector and the detector and also uniquely preassigning the direction of magnetization in each of them. In the lateral spin valve as shown in Fig. 1, the direction of magnetization of the contacts can be changed by means of an external magnetic field directed along their easy-magnetization axis. The contacts having the same length but a different width possess different anisotropy fields and their magnetization reversal occurs in different fields. For our devices, the contacts F1 and F2 were fabricated with a width of $w = 6\,\mu$m, and the contacts F3, F4, F5, and F6 had a width of $w = 4\,\mu$m.

For the contacts F1 and F6, the current-carrying paths were set at both ends, which made it possible to measure anisotropic magnetoresistance (AMR) in these contacts. The results of the AMR measurements for the contacts of different widths w are shown in Fig. 4. When sweeping the magnetic field B_y applied in the direction of the y axis from -1 to $+1$ kG and back, the magnetization reversal of the "broad" ($w = 6\,\mu$m) contact occurred in a field of the order of ±40 G, and the "narrow" one ($w = 4\,\mu$m) in the field of ±50 G.

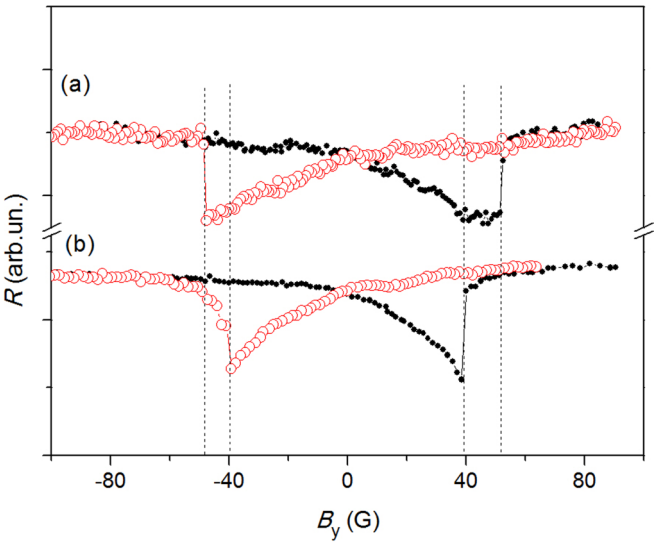

FIG. 4. (a) AMR of the contact F6 with a width of 4 μm. (b) AMR of the contact F1 with a width of 6 μm. A magnetic field lies in the contact plane and is directed along their long axis. Light large circles denote a decrease of the field from positive values through zero to negative values. Dark shallow circles are the sweeping of the field in the opposite direction. The vertical dotted line segments indicate the magnetic field values at which the magnetization reversal of the contacts occurs.

Also, the longitudinal and transverse magnetizations of the contacts (along the y and x axes) during their magnetization reversal by the field B_y were investigated by optically measuring the Kerr effect. Captured with a Kerr microscope, the images of the contacts contained alternating different-contrast lines oriented across the long contact axes. The appearance and intensification of the contrast of these lines are correlated with the behavior of AMR.

The above-given data evidence of emerging a transverse component of magnetization in the device's contacts in some sections of the magnetic field scale as magnetization reversal occurs. It should be emphasized that the regions with transverse magnetization are observed in narrow contacts at magnetic field values close to the magnetization reversal field of the broad contacts. Thus, the state of the magnetization of the contacts in the region of the magnetization reversal fields cannot be unambiguously interpreted as homogeneous. As a consequence, the experiments to measure spin effects during magnetization reversal of ferromagnetic contacts by the magnetic field in the lateral spin valves at hand cannot yield reliable results.

On the other hand, the contacts magnetized to saturation in a magnetic field of the order of 1 kG preserve their parallel magnetization even after reducing the field to zero. In this case, it is convenient to control the direction of the electrons magnetization by a transverse magnetic field, as it happens under the Hanle effect conditions. If this field is smaller than the transverse field of the anisotropy of the contact, its influence on the longitudinal magnetization of the contacts is negligible. Then, the angle between the magnetization directions of the electron gas and detector changes due to the Larmor precession of the electron spin.

From expressions (15)–(17) it follows that, for the current $I < 0$, the spin signal V_D is negative for parallel magnetization of the contacts and positive for the antiparallel one. When reversing the current direction, the spin signal must also change only the sign; its absolute value must remain unchanged. It should be noted that this assertion holds for the low-current approximation, i.e., when the electron diffusion rate is much greater than the electron drift velocity and the spin current flowing towards the detector from the injector is equal to half the electron spin current flowing through the injector. Thus, in the low-current regime, the experiments with a change in the direction of the electric current through the injector are equivalent to the experiments with a change in the direction of magnetization of the contacts.

The output signal V_E registered directly from the contact detector is shown in Fig. 5(a) with small circles. The signal V_E can be represented as a superposition of two contributions, which differ significantly from each other both in amplitude and in dependence on the magnetic field. One of these contributions V_H, with amplitudes from fractions to unities of microvolts, may be interpreted as being associated with the spin transport, i.e., as being due to the Hanle effect whose dependence on the magnetic field is described by expression (17). The second contribution is the background signal V_B with amplitude from a few to tens of microvolts and it demonstrates a quadratic magnetic field dependence. This signal is caused by spreading of the charge current throughout the semiconductor [11], and its dependence on the magnetic field is governed by the field dependence of the semiconductor resistance. Figure 5(a) shows this signal with a dashed line.

In Fig. 5(b) the circles show the spin signal V_H for the injector current $I = -16\,\mu$A, obtained by subtracting the background signal V_B from the initial V_E. The triangles and squares display the spin signals for the currents $I = -4$ and $-8\ \mu$A. They also represent the difference between the appropriate initial and background signals. The solid lines are graphs of the voltage $V_D(B,d)$ calculated using expression (17). In these calculations, we set the following parameters into expression (15), taking into account the P_S dependencies on the current (17): the values of the ferromagnetic contact sizes, the distances between their central axes d, the temperature $T = 77$ K, the value of the injector current I, and the g factor of electrons in InSb $g = -52$. The electron gas was considered as nondegenerate. The L_S, T_S, and P_J were varied parameters determined by fitting of the theoretical curve (17) to the experimental data.

The magnitude of the spin relaxation time T_S mainly affects the width of the signal line in expression (15). The magnitude L_S can be estimated from the dependence of the maximum value of the spin signal on the distance between the same injector (e.g., F2) and different detectors (e.g., F3 and F4).

The Hanle spin signal measured when $B = 0$ yields a maximum signal. Figure 5(c) illustrates the Hanle signals for the detectors F3 and F4 whose central axes are spaced from the injector F2 by 11 and 21 μm, respectively. The current I is -11 μA.

As for the detector of the width of 4 μm (F4), in the current range from -3 to -20 μA we succeeded in describing the entire set of the experimental data with sufficient accuracy by the same parameters such as $L_S = 25\ \mu$m, $T_S = 1.5$ ns, and

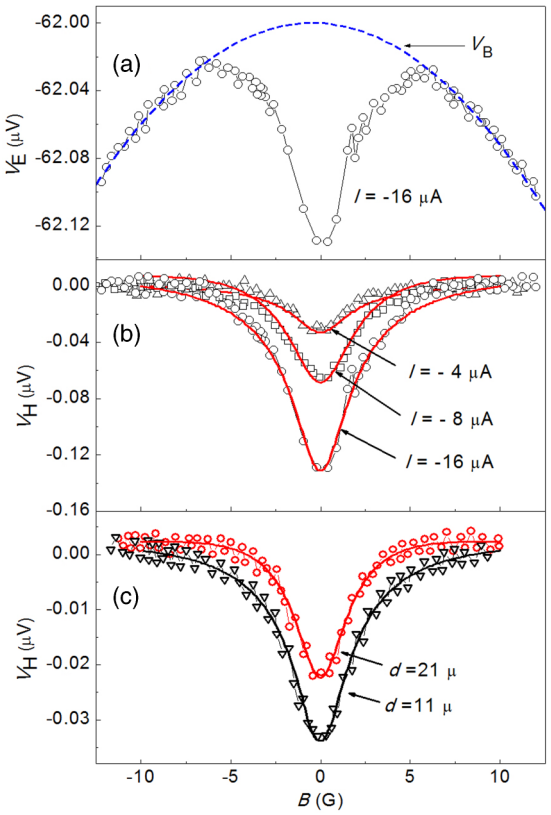

FIG. 5. (a) Circles: the experimental voltage V_E between F5 and F6 as a function of B. The current $I = -16\,\mu$A flows through the injector F4 and the contact F1 (see Fig. 3). The temperature is $T = 77$ K. The dashed line is the background signal V_B approximated by a second-order polynomial.(b) Symbols denote the curves for the Hanle signal $V_H = V_E - V_B$ calculated as the difference between the experimentally measured voltage V_E and the background signal V_B. The solid lines were calculated using expressions (15) and (17). The distance between F4 and F5 is equal to $d = 10\,\mu$m (see Fig. 3); other parameters are $T_S = 1.5$ ns, $L_S = 25\,\mu$m, $P_J = 0.06$, $T = 77$ K. (c) Triangles: The voltage V_H registered by the detector F3 spaced 11 μm apart from the injector F2. Circles: The voltage V_H registered by detector F4 spaced 21 μm apart from F2. The solid lines depict the voltages $V\ (B, d)$ calculated using the expressions (15) and (17) for $I = -11\,\mu$A, $T_S = 1.5$ ns, $L_S = 25\ \mu$m, $P_J = 0.02$, $T = 77$ K, and $d = 11$ and 21 μm, respectively.

$P_J = 0.06$. The data calculated are in good agreement with the experimental ones [Fig. 5(b), solid lines].

Figure 6(a) presents the graphs of the voltage dependence on the detector F3 on a magnetic field for the forward and reverse current I in the injector F2. Figure 6(b) depicts the Hanle effect signals obtained by subtracting the corresponding background signals $V1_B$ and $V2_B$ from the measured ones. The Hanle effect signals obtained for opposite directions of the current are a mirror image of each other relative to the level of $+0.009\,\mu$V.

The resulting value $T_S = 1.5$ ns can be compared with the transverse spin relaxation time T_2 obtained by electron spin resonance (ESR). In InSb with the electron density $n = 2\times10^{14}$ cm^{-3} at $T = 4.2$ K, the ESR linewidth of the conduction electrons is $\Delta H = 2$Oe [21]. This corresponds

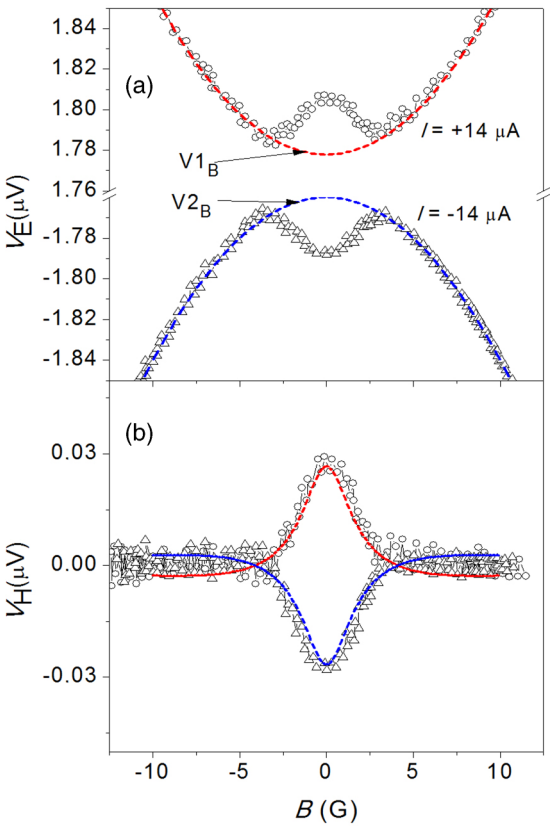

FIG. 6. (a) Voltage V_E, measured on the detector F3 with respect to the contact F6. The current I passes through the injector F2 and the contact F1. Light circle indicate the current $I = +14\,\mu$A; light triangles show the current $I = -14\,\mu$A. Dotted lines denote an approximation of background signals by polynomials of the second order. (b). The Hanle effect signals obtained by subtracting background signals from the original ones, $V_H = V_E - V_B$. Dotted lines show calculations using expressions (17) with the following parameters: $T_S = 1.5$ ns, $L_S = 25\,\mu$m, $P_J = 0.02$, $T = 77$ K, and $d = 11\,\mu$m. The upper curve is the current $I = +14\,\mu$A, the lower curve is the current $I = -14\,\mu$A.

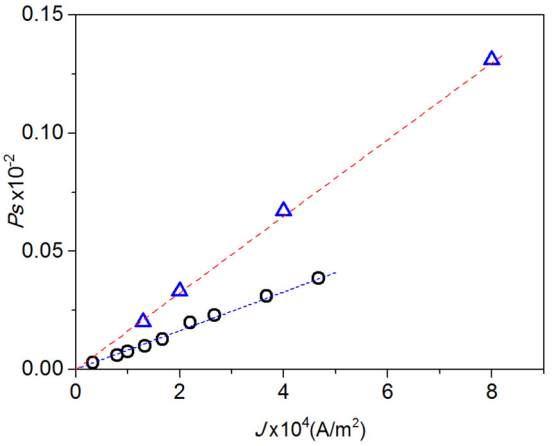

FIG. 7. The spin polarization P_S under the injecting ferromagnetic contact as a function of the electric current density J_C. The unfilled triangles indicate the polarization under the injector F4; the dashed line parametrizes the values of P_S depending on J_C in accordance with formula (16); the parameter of the spin-injection efficiency is equal to $P_J = 0.06$. The open circles denote the polarization under injector F2, the parameter of the spin-current efficiency is $P_J = 0.02$.

to the transverse spin relaxation time $T_2 = 6.5$ ns. Given the tendency of the spin relaxation time to reduce with increasing temperature, the as-obtained value of $T_S = 1.5$ ns at $T = 77$ K satisfactorily correlates with the value of T_2 calculated based on the ESR data at $T = 4.2$ K.

From the measurements of the signals under the Hanle effect, we arrived at the value of $L_S = 25\,\mu$m for InSb. It is significantly (4–6 times) greater than the spin diffusion length in GaAs, where L_S ranges from 6 [12] to 3 μm [11]. This fact can be explained by higher electron mobility (by two orders of magnitude) in InSb than in GaAs [16]. Indeed, the spin diffusion length is $L_S = \sqrt{DT_S}$. The mobility μ and the diffusion coefficient D are related by Einstein's relation that nondegenerate electrons have the form $D = \frac{k_B T}{e}\mu$. Hence, $L_S \sim \sqrt{\mu T_S}$. The time T_S measured in InSb is about 3 times less than in GaAs [12]. Thus, the spin diffusion length in InSb is about 6 times higher than in GaAs, which is in good agreement with our measurements. It should also be noted that the magnitude of L_S depends not only on mobility and temperature but also on imperfection and other individual features of the samples. The review [18] shows that the value of the parameter L_S measured by different groups of researchers for different samples of the same material can vary by tens of times.

Figure 7 shows the values of the electron spin polarization P_S in the semiconductor under the injecting ferromagnetic contact obtained from Eqs. (15)–(17). They are a function of the injected electric current density for two different contacts. The unfilled triangles represent the injector F4 (4 μm wide) and the detector F5, the open circles correspond to the injector F2 (6 μm wide) and the detector F3 (see Fig. 3). Within the measurement error, the dependence of the electron spin polarization P_S on the injection current density is a linear function. For the injector F4 the parameter of the spin-current injection efficiency amounts to $P_J = 0.06$. For the injector F2, all the P_S values calculated for different currents are well described by one and the same value of $P_J = 0.02$.

The findings mentioned above demonstrate that the spin-current injection efficiency P_J for two contacts of one and the same device may differ noticeably.

One of the possible reasons for the difference observed appears to be an error in determining P_S. Perhaps this error is caused by the assumption of the contact width smallness compared to the distances between the contacts when processing the experimental data. In fact, the contact widths are comparable with the distances between the contact edges. This circumstance makes it necessary to carry out the averaging process over the contact width. This procedure results in the appearance of a systematic error in determining P_J. The wider the contact, the greater is the inaccuracy. Emanating from the foregoing, in what follows, the true value of the injection efficiency P_J is assumed to lie between the values computed for the different contacts F2 and F4. Thus, the value of the injection efficiency P_J for the system under study (InSb/MgO/$Co_{0.9}Fe_{0.1}$) is equal to $P_J = 0.04 \pm 0.02$.

Another possible reason for the above-described difference in the values of P_J for different injectors may be attributed to a very strong dependence of P_J on the presence and properties of the MgO interlayer at the ferromagnetic injector-semiconductor boundary. Let us discuss the role of the MgO dielectric layer for reaching the above injection efficiency P_J. In doing so, we compare this value to the value predicted by the standard theory of injection [7]. The value of P_J for a "transparent" ferromagnetic metal/semiconductor contact, when the contact resistance is less than the resistance of the semiconductor and ferromagnetic, can be represented as

$$P_J^{(\mathrm{tr})} \sim \frac{\rho_\mathrm{F}}{\rho}\frac{L_\mathrm{S}^{(\mathrm{F})}}{L_\mathrm{S}} P_S^{(\mathrm{F})}, \tag{19}$$

where ρ and ρ_F are the specific resistances of the semiconductor and ferromagnetic metal, respectively; L_S and $L_\mathrm{S}^{(\mathrm{F})}$ are their spin diffusion lengths. As for the InSb crystal used in the experiment, its electron density is $n = 1.2\times10^{14}\,\mathrm{cm}^{-3}$, its electron mobility is $\mu = 6.2\times10^5\,\mathrm{cm}^2/\mathrm{Vs}$ at $T = 77\,\mathrm{K}$, the specific resistance is $\rho = 1/e\mu n = 0.084\ \Omega$ cm, and the experimental spin-diffusion length amounts to $L_\mathrm{S} = 25\,\mu$m. As for the ferromagnet close to the $Co_{0.91}Fe_{0.09}$ composition, its spin-diffusion length is $L_S^{(\mathrm{F})} = 0.012\,\mu$m and its specific resistance reaches $\rho_\mathrm{F} = 7\times10^{-6}\,\Omega\,\mathrm{cm}$ at a temperature of 4.2 K [22]. Next, to estimate the injection efficiency P_J for the transparent contact, we admit that the magnitude order of $L_\mathrm{S}^{(\mathrm{F})}$ and ρ_F measured at $T = 77\,\mathrm{K}$ remains unchangeable with increasing temperature. Then the upper estimate comes to $P_J^{(\mathrm{tr})} \leqslant 4\times10^{-8}$.

The previously mentioned estimates show that the use of the MgO tunnel barrier for an enhancement of the efficiency of the spin injection from the ferromagnetic metal into the InSb semiconductor enables one to increase this efficiency by 6 orders of magnitude compared with the theoretically calculated efficiency of the $InSb/Co_{0.9}Fe_{0.1}$ transparent contact without a tunnel layer. Being strongly dependent on the presence of the MgO tunnel barrier, the value of P_J is extremely sensitive to the quality of a very thin MgO layer. Even a little difference in the tunnel properties of the MgO layer between the semiconductor and different ferromagnetic contacts can lead to a well-marked difference in the efficiency of the spin injection P_J for these contacts.

In spite of differing in the parameters of the spin injection efficiency P_J of different contacts from each other, from Eq. (16) we can extract information about the system characteristic dependent to a much lesser extent on the properties of the particular contact. As such a characteristic, the ratio P_S/P_J can be used. According to (16), the ratio is directly proportional to the density of the electric current flowing through the contact injector, with the proportionality coefficient depending on the characteristics of the semiconductor and the width of the contact w:

$$P_S/P_J = J_C/\mathcal{J}_C, \tag{20}$$

where

$$\mathcal{J}_C = 2\,enD/w. \tag{21}$$

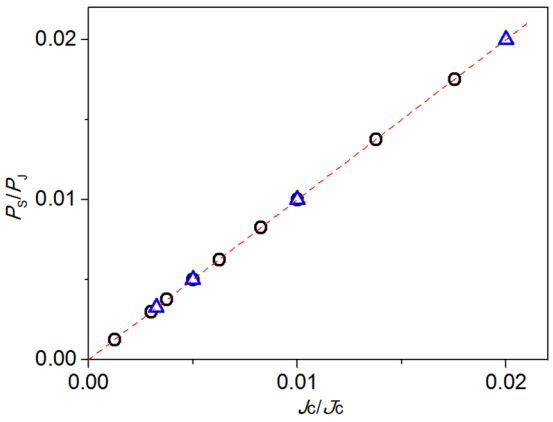

FIG. 8. Dependence of the ratio of the polarizations (P_S/P_J) on the ratio of the current densities ($J_C/\mathcal{J}_C$). Circles and triangles denote the injectors with a width of 6 and 4 μm, respectively.

Figure 8 represents these data in the coordinates (P_S/P_J) vs ($J_C/\mathcal{J}_C$). With such a choice of the variables, the experimental data for P_S of all the injector-detector pairs lie in one and the same straight line: unfilled triangles represent the injector F4 (4 μm wide) and the detector F5, the open circles correspond to the injector F2 (6 μm wide) and the detector F3. For the entire current range ($J_C \ll \mathcal{J}_C$), the spin polarization P_S is significantly less than the value of the current polarization P_J. The smallness of the obtained values of P_J as compared to the ferromagnetic polarization $P_S^{(\mathrm{F})} \approx 0.224$ may be due to two reasons.

Apparently, one of them is the imperfect MgO tunnel barrier at the interface of the InSb semiconductor plate with the ferromagnetic contacts. This is associated with defects in the structure of the MgO layer. The defects of the tunnel barrier result in a decrease in its resistance and the manifestation of the conductivity mismatch effect [4] for the contact pair $Co_{0.9}Fe_{0.1}$-InSb.

Another reason may be revealed even in case of a highly perfect tunnel barrier with high resistance which minimizes the conductivity mismatch effect. Such a contact can provide a significant effect only if the tunneling layer acts as an effective spin filter. The latter must transmit electrons with one spin direction and reflect a significant portion of the electrons with an opposite spin direction. These properties of the tunnel junction are predetermined by the relation of the energy spectrum parameters of the ferromagnetic CoFe and MgO on the one hand and by InSb and MgO on the other hand. However, a detailed discussion of these reasons is beyond the scope of this work.

V. CONCLUSIONS

The basic relations of the theory of spin-charge coupling for complete description of electric detection of nonequilibrium spin density of the electrons injected into a semiconductor with ferromagnetic metal contacts are formulated in the present paper. The analytical expressions have been derived for the electrical response of the ferromagnetic contact on a spin disturbance in a semiconductor with an arbitrary dispersion law of electrons and an arbitrary degree of degeneracy of the electron gas.

The authors discuss a scheme of nonlocal electrical detection of spin transport implemented in an InSb nondegenerate semiconductor with $Co_{0.9}Fe_{0.1}$ ferromagnetic contacts under the Hanle effect conditions. The foregoing allows one to determine the spin diffusion length, the spin relaxation time and the current injection efficiency, and also to calculate the magnitude of polarization of the electron gas under an injector as a function of the injection current.

The use of an MgO dielectric layer between the InSb semiconductor and the CoFe metal contact increases the current injection efficiency. In our case, this increase is 6 orders of magnitude in comparison with the current injection efficiency of a transparent contact. However, the spin injection efficiency does not reach the values comparable with polarization in a ferromagnet. One of possible reasons for that is imperfectness of the MgO layer, as well as a negligible performance of the spin filter in the MgO layer that separates the CoFe metal and the InSb semiconductor.

ACKNOWLEDGMENTS

The research has been carried out within the state assignment on the theme "Spin," number 01201463330 (Project 15-17-2-17) with the support of the Ministry of Education and Science of the Russian Federation (Grant No. 14.Z50.31.0025) and RFBR (Grant No. 16-02-00044).

[1] S. Datta and B. Das, Appl. Phys. Lett. **56**, 665 (1990).
[2] V. V. Osipov and A. M. Bratkovsky, Appl. Phys. Lett. **84**, 2118 (2004).
[3] H. X. Tang, F. G. Monzon, M. L. Roukes, F. J. Jedema, A. T. Filip, and B. J. van Wees, in *Semiconductor Spintronics and Quantum Computation*, edited by D. D. Awschalom, D. Loss, and N. Samarth (Springer, Berlin, 2002), pp. 31–87.
[4] G. Schmidt, D. Ferrand, L. W. Molenkamp, A. T. Filip, and B. J. van Wees, Phys. Rev. B **62**, R4790(R) (2000).
[5] A. Fert and I. A. Campbell, J. Phys. **32**, C1-46 (1971).
[6] E. I. Rashba, Phys. Rev. B **62**, R16267(R) (2000).
[7] J. Fabian, A. Matos-Abiague, C. Ertler, P. Stano, and I. Zutić, Acta Phys. Slov. **57**, 565 (2007).
[8] M. Johnson and R. H. Silsbee, Phys. Rev. Lett. **55**, 1790 (1985).
[9] M. Johnson and R. H. Silsbee, Phys. Rev. B **37**, 5312 (1988).
[10] F. J. Jedema, H. B. Heersche, A. T. Filip, J. J. A. Baselmans, and B. J. van Wees, Nature (London) **416**, 713 (2002).
[11] X. Lou, C. Adelmann, S. A. Crooker, E. S. Garlid, J. Zhang, S. M. Reddy, S. D. Flexner, C. J. Palmstrøm, and P. A. Crowell, Nat. Phys. **3**, 197 (2007).
[12] M. Ciorga, A. Einwanger, U. Wurstbauer, D. Schuh, W. Wegscheider, and D. Weiss, Phys. Rev. B **79**, 165321 (2009).
[13] O. M. J. van't Erve, A. L. Friedman, E. Cobas, C. H. Li, J. T. Robinson, and B. T. Jonker, Nat. Nanotechnol. **7**, 737 (2012).
[14] N. A. Viglin, V. V. Ustinov, V. M. Tsvelikhovskaya, and T. N. Pavlov, JETP Lett. **101**, 113 (2015).
[15] M. Holub and P. Bhattacharya, J. Phys. D: Appl. Phys. **40**, R179 (2007).
[16] E. Litwin-Staszewska, W. Szymanska, and R. Piotrzkowski, Phys. Status Solidi (b) **106**, 551 (1981).
[17] N. A. Viglin, V. V. Ustinov, and V. V. Osipov, JETP Lett. **86**, 193 (2007).
[18] J. Bass and W. P. Pratt Jr., J. Phys.: Condens. Matter **19**, 183201 (2007).
[19] A. I. Liechtenstein, V. I. Anisimov, and J. Zaanen, Phys. Rev. B **52**, R5467(R) (1995).
[20] O. K Andersen and O. Jepsen, Phys. Rev. Lett. **53**, 2571 (1984).
[21] G. Bemski, Phys. Rev. Lett. **4**, 62 (1960).
[22] A. C. Reilly, W. Park, R. Slater, B. Ouaglal, R. Loloee, W. P. Pratt, and J. Bass, J. Magn. Magn. Mater. **195**, L269 (1999).